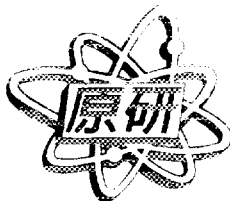


**JAERI-Research**  
**97-070**



JP9711012



**ESSENTIAL TECHNOLOGIES FOR DEVELOPING HUMAN  
AND ROBOT COLLABORATIVE SYSTEM**

**October 1997**

**Nobuyuki ISHIKAWA and Katsuo SUZUKI**

**29-03**

*d*

**日本原子力研究所**  
**Japan Atomic Energy Research Institute**

本レポートは、日本原子力研究所が不定期に公刊している研究報告書です。  
入手の問い合わせは、日本原子力研究所研究情報部研究情報課（〒319-11 茨城県那珂郡東海村）あて、お申し越してください。なお、このほかに財団法人原子力弘済会資料センター（〒319-11 茨城県那珂郡東海村日本原子力研究所内）で複写による実費頒布をおこなっております。

This report is issued irregularly.

Inquiries about availability of the reports should be addressed to Research Information Division, Department of Intellectual Resources, Japan Atomic Energy Research Institute, Tokai-mura, Naka-gun, Ibaraki-ken, 319-11, Japan.

© Japan Atomic Energy Research Institute, 1997

編集兼発行 日本原子力研究所  
印 刷 いばらき印刷(株)

**Essential Technologies for Developing Human and  
Robot Collaborative System**

**Nobuyuki ISHIKAWA and Katsuo SUZUKI**

**Department of Reactor Engineering  
Tokai Research Establishment  
Japan Atomic Energy Research Institute  
Tokai-mura, Naka-gun, Ibaraki-ken**

**(Received September 9, 1997)**

In this study, we aim to develop a concept of new robot system, i.e., " human and robot collaborative system " , for the patrol of nuclear power plants. This paper deals with the two essential technologies developed for the system. One is the autonomous navigation program with human intervention function which is indispensable for human and robot collaboration. The other is the position estimation method by using gyroscope and TV image to make the estimation accuracy much higher for safe navigation. Feasibility of the position estimation method is evaluated by experiment and numerical simulation

**Keywords: Human and Robot Collaboration, Autonomous Navigation Program,  
Position Estimation**

人間・ロボット協調システム開発のための要素技術

日本原子力研究所東海研究所原子炉工学部

石川 信行・鈴木 勝男

(1997年9月9日受理)

本研究においては、原子力プラント巡回点検作業のために、新しい概念のロボットシステム、「人間・ロボット協調システム」を開発することを目的としている。本論文では、そのために開発した2つの要素技術（自律走行プログラム、ロボット自己位置推定法）およびシステムの基本概念について述べる。開発した自律走行プログラムは、従来の自律移動ロボットの走行プログラムに、人間協調動作で必要となる随時割込み機能を付加することにより実現した。また、高精度な自己位置推定法を実現するために、ジャイロとテレビ画像を用いた方法を提案し、その実用可能性を実験ならびに数値シミュレーションで評価した。

## Contents

1. Introduction .....	1
2. The Proposition of a Human and Robot Collaborative System.....	3
3. Development of Autonomous Navigation Program for Human and Robot Collaboration .....	5
3.1 System Configuration .....	5
3.2 Autonomous Navigation Program.....	6
4. Technologies for the Positioning of a Mobile Robot.....	8
4.1 Position Estimation Using Odometry and Gyroscope.....	8
4.1.1 Combinatorial Use of Odometry and Gyroscope.....	8
4.1.2 Experimental Results .....	10
4.2 Correction of Position Estimation Error by Using TV Image Deviation .....	13
4.2.1 Principle .....	13
4.2.2 Results of Numerical Simulation .....	16
4.3 Positioning Tool.....	17
5. Conclusions .....	19
Acknowledgments.....	19
References .....	20

## 目 次

1. はじめに .....	1
2. 人間・ロボット協調システムの提案 .....	3
3. 人間・ロボット協調のための自律走行プログラム開発 .....	5
3.1 システム構成 .....	5
3.2 自律走行プログラム .....	6
4. 移動ロボットの位置推定技術 .....	8
4.1 ジャイロとオドメトリによる位置推定 .....	8
4.1.1 ジャイロとオドメトリの併用法 .....	8
4.1.2 実験結果 .....	10
4.2 画像偏差を用いた位置推定誤差の補正法 .....	13
4.2.1 原 理 .....	13
4.2.2 数値シミュレーション結果 .....	16
4.3 ポジショニングツール .....	17
5. む す び .....	19
謝 辞 .....	19
参考文献 .....	20

## 1 Introduction

Autonomous mobile robots are widely studied in the robotics research field to realize a self-consistent system for performing given tasks in unstructured environments. Although the self-consistent autonomous system has an advantage of reducing the labor of human, it is not always suitable to use this system for the tasks in nuclear power plants. For the inspecting patrol of nuclear power plants, we propose a human and robot collaborative system with the high safety and reliability. A basic idea of this system is that in the normal situation the robot takes an autonomous action, while in the abnormal situation when an unexpected problem occurred human operators act to help the robot solve the problem. Thereby the system is incorporated with the ability to cope with the abnormal event. The system is constructed by adding an interfacing function between human and robot to an ordinary autonomous system. This paper focuses on key technologies in realizing the human and robot collaborative system and position estimation techniques with high accuracy which is essential to robot navigation.

The system is composed of two parts: a host engineering workstation(EWS) and a mobile robot system. In this study, we utilize the “yamabico” system[1] as a mobile robot system, which is developed for autonomous robot experiments in the intelligent robotics laboratory of Tsukuba university. To meet our requirements the original system programs of the “yamabico” have been modified by adding a server program and an autonomous navigation program. The server program is composed of a set of service routines for communication between host EWS and robot system in transmitting data and commands for robot operation. The autonomous navigation program mainly manages switching of navigation modes (i.e., autonomous and manual modes), whose function is essential to human and robot collaborative navigation. This is realized by incorporating the programming technique of the process control. We developed a system of commands for robot navigation and navigation mode control.

A position estimation technique, based on combinatorial use of an odometry and gyroscope, is studied. The data of gyroscope is used to correct a sudden odometric error (e.g. slip of the wheel) and the drift of gyroscope is compensated by lowpass

filtering. To make the above-mentioned position estimation more accurate, we present another error correction method by utilizing TV image. These positioning methods are integrated as “positioning tool” on the host EWS.

This paper is organized as follows. In chapter 2 we explain the proposed human and robot collaborative system focusing on the roles of human operator and autonomous robot. The schematic description of the system and the key technologies required for developing the system are presented in chapter 3. The positioning methods and “positioning tool” are described in chapter 4. Summary and conclusions are in chapter 5.



## 2 The Proposition of a Human and Robot Collaborative System

A general trend on the autonomous robotics research is to develop a complete self-consistent autonomous robot system, being expected to perform some given tasks under unfixed conditions. In order to incorporate the autonomy in the robot system, however, high level reasoning techniques such as artificial intelligence have to be adopted. We have some misgivings about introducing such robot system into nuclear power plants, since in the nuclear facilities we have to place careful consideration on safety, reliability and ability of taking an urgent action in emergency. Considering these points, our research is addressed to two techniques; (a) complete autonomous mobile robot for normal conditions and (b) human and robot collaborative technique for emergency.

In the complete self-consistent autonomous robot system, the robot takes an autonomous action directed by the program implemented in advance. When we want the robot to take a fully autonomous action for unexpected events, we have to provide such a sophisticated problem solving algorithm as an obstacle avoidance applicable to any unknown environment. The state-of-arts suggests that it is almost impossible to develop the above mentioned algorithm, and that it is required to re-implement the programs depending on the change of environment. This results in the reduction of much amount of efficiency, reliability and rapidity in performing tasks. For this reason, we study the human and robot collaborative system, in which human intervention copes with the unexpected events, and thereby the efficiency, reliability and rapidity are considerably enhanced. The system development approach is to add the interface function of the human intervention to the conventional autonomous robot system. Key technologies of the system is described in the next chapter.

Table 2.1 Roles of human and robot.

	robot	human
normal	autonomous action	monitor the robot action
abnormal	slave (serve sensor data)	master (operate the robot)

In Table 2.1, the roles of human and robot in this system are shown [2]. We define the states of the system: “normal” and “abnormal”. “Normal” state is the state that the values measured by external sensor coincide with the values estimated from the environment model within a prescribed range. On the contrary, “abnormal” state is that the measured values deviate from the estimated ones and also an abnormal motion of the robot is observed. To be brief, the proposed system is a new robot system to make efficient use of human intelligence and artificial intelligence for the inspecting patrol of nuclear power plants.

### 3 Development of Autonomous Navigation Program for Human and Robot Collaboration

#### 3.1 System Configuration

Figure 3.1 depicts a schematic diagram of the system. It is composed of two parts of hardware: the host engineering workstation(EWS) and the mobile robot system. As the host EWS we utilize the SiliconGraphics Onyx since it has a high performance of processing graphics to build the convenient graphical user interface(GUI). The mobile robot system is realized by adopting the “yamabico” system, which is a small size mobile robot for autonomous robot experiments. A hardware interconnecting between the host EWS and the mobile robot system is wireless modem through which the sensor data obtained by inspection activity and commands issued by operator are transmitted.

The server program on the robot system is composed of a set of service routines for communication between the host EWS and the robot system in transmitting the data and commands for robot operation. The autonomous navigation program of the robot system mainly manages switching of the navigation modes (i.e., autonomous and manual modes). This function is essential to human and robot collaborative navigation.

The GUI, implemented on the host EWS, is a software interface between human and robot. The GUI is a group of “tools” which is a set of separated modules related to the respective functions. Namely this group of “tools” include “positioning tool”, “path generation tool” and “manual robot operation tool”. In the next chapter, details of the “positioning tool” is presented.

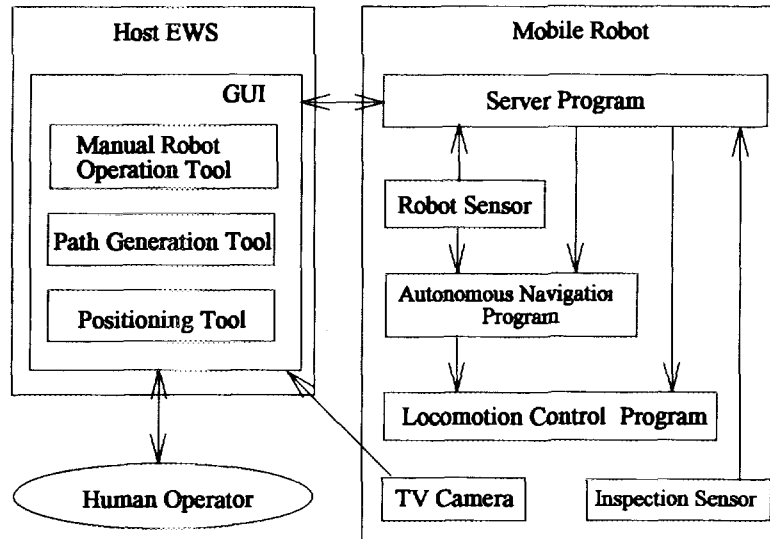


Fig. 3.1 Configuration of a human and robot collaborative system

### 3.2 Autonomous Navigation Program

In this section, the autonomous navigation program, being modified for the human and robot collaborative system, is explained. Modification is made in the original autonomous navigation program of “yamabico” to incorporate the function of human intervention. The modified program has functions of; (a) systematic switching between autonomous and manual navigation modes, and (b) restarting the autonomous navigation after manual operation. The mode switching function is attained by the use of programming techniques of process control. In this program, each mode is regarded as a process. To control the mode, we introduce some process control commands to this program. To realize the function of restart, we introduce some navigation commands to achieve a single robot action unit (e.g. go to  $(x,y)$  and keep  $\theta$ ) with navigation commands ( $go\ x\ y\ \theta$ ). A schematic diagram of the autonomous navigation program is depicted in Figure 3.2.

The autonomous navigation path is given by a sequence of navigation commands in this program. And the interrupt handler controls the switching actions according to the process control commands issued by a human operator. For human

intervening, the process control command suspends the autonomous navigation and restart the suspended command of autonomous navigation or restart the navigation command which is directed by the operator from the preceding command sequence. Commands of the autonomous navigation program are listed in Table 3.1.

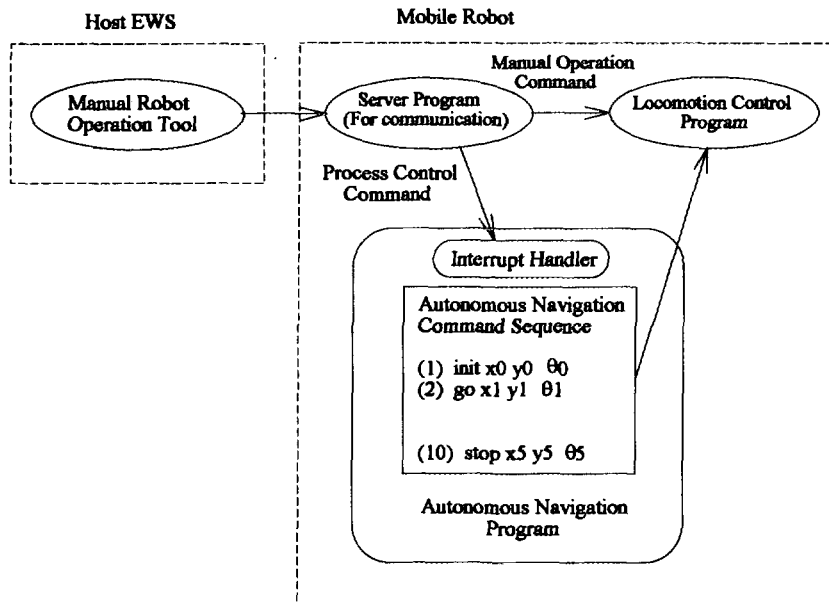


Fig. 3.2 Schematic description of autonomous navigation program

Table 3.1 Commands of autonomous navigation program

• Navigation commands

command	explanation
init x y $\theta$	set the robot position as (x,y, $\theta$ ) of world coordinate system.
stop x y $\theta$	move the robot to (x,y, $\theta$ ) and stop.
go x y $\theta$	move the robot to (x,y, $\theta$ ) and execute next command if the robot arrives at (x,y, $\theta$ ).

• Process control commands

command	explanation
INITIAL	initialization of autonomous navigation program.
SET_NAVI_COMMAND ***	set the navigation commands sequence (***)
PAUSE	pause the autonomous navigation.
RESTART_CURRENT	restart the autonomous navigation from suspended command.
RESTART_OTHER n	restart the autonomous navigation from other command order n-th.

## 4 Technologies for the Positioning of a Mobile Robot

### 4.1 Position Estimation Using Odometry and Gyroscope

#### 4.1.1 Combinatorial Use of Odometry and Gyroscope

The estimation of robot position is very important for safe navigation. Odometry is ordinarily utilized for the position estimation by integrating the amount of wheel rotations. The estimation error in odometry is classified into two types: one is “stationary error”, and the other is “sudden error”. The stationary error is caused by the variation of kinematics parameter such as distance between wheels. On the other hand, sudden error is caused by the instantaneous events such as a slip of the wheel. By using a gyroscope, the sudden error can be corrected easily [3][4].

Let us obtain wheel’s angular velocities  $u_R(k)$  and  $u_L(k)$  by the encoder mounted on the axle. Then we can calculate the position and the orientation of the robot as follows (Figure 4.1):

$$\Omega(k) = \frac{L[u_R(k) - u_L(k)]}{T} \quad (1)$$

$$v(k) = \frac{L[u_R(k) + u_L(k)]}{2} \quad (2)$$

$$\theta(k+1) = \theta(k) + \tau\Omega(k) \quad (3)$$

$$x(k+1) = x(k) + \tau v(k) \cos \theta(k) \quad (4)$$

$$y(k+1) = y(k) + \tau v(k) \sin \theta(k) , \quad (5)$$

where  $\tau$  denotes the estimation period,  $x(k)$  and  $y(k)$  are estimated positions and  $\theta(k)$  is the orientation angle.  $L$  is a wheel radius,  $T$  is a distance between wheels,  $\Omega(k)$  is the rotational angular velocity and  $v(k)$  is the velocity.

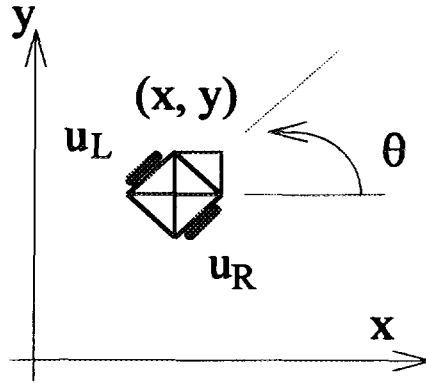


Fig. 4.1 Model of mobile robot for position estimation

A slip results in the error of  $\Omega(k)$ . In the presented positioning method, the angular velocity  $\Omega(k)$  by odometry is basically used. However, the angular velocity measured by the gyroscope is used in stead of the  $\Omega(k)$  in the case of the sudden error occurrence. We introduce the following quantity as a criteria of the sudden error occurrence:

$$\Delta(k) = \Omega_{\text{gyro}}(k) - \Omega_{\text{odom}}(k), \quad (6)$$

where,  $\Omega_{\text{gyro}}(k)$  denotes the rotational angular velocity measured directly by the gyroscope and  $\Omega_{\text{odom}}(k)$  is calculated by Eq.(1). Since the absolute value of  $\Delta(k)$  becomes larger when a slip is occurred, the occurrence of slip can be known. By setting the threshold value  $\Delta_{\text{max}}$  for  $\Delta(k)$ , we determine  $\Omega(k)$  as

$$\Omega(k) = \begin{cases} \Omega_{\text{odom}}(k) & (|\Delta(k)| \leq \Delta_{\text{max}}) \\ \overline{\Omega}_{\text{gyro}}(k) & (|\Delta(k)| > \Delta_{\text{max}}) \end{cases}, \quad (7)$$

where  $\overline{\Omega}_{\text{gyro}}(k)$  is the drift-compensated rotational angular velocity.

Next we proceed to the method of drift compensation. We present a drift

compensation method based on a lowpass filtering technique. The amount of  $\Delta(k)$  includes the sudden error and the drift of gyroscope. A frequency analysis reveals that the component of  $\Delta(k)$  caused by sudden error belongs to high frequency domain and that by drift to low frequency domain. This suggests us the possibility of detecting the drift component by the use of a lowpass filter. Considering the stability of the filtering operation we adopt a FIR digital lowpass filter. Let  $H(z^{-1})$  denote the transfer function of digital filter, then the drift of gyroscope is estimated as

$$\bar{\Delta}(k) = H(z^{-1})\Delta(k) \quad (8)$$

where  $H(z^{-1}) = h_0 + h_1z^{-1} + \dots + h_Nz^{-N}$ . The angular velocity measured by the gyroscope with drift compensation is given by

$$\bar{\Omega}_{\text{gyro}}(k) = \Omega_{\text{gyro}}(k) - \bar{\Delta}(k). \quad (9)$$

#### 4.1.2 Experimental Results

We present the experimental results of the position estimation method described in the previous section. In the experiment, we moved the robot straight by 1800[mm], and on the way at 900[mm] we lifted up its left wheel during a very short period in order to simulate a sudden slip artificially. Figure 4.2 shows the rotational angular velocity by the gyroscope. We can see the bias drift of about 1[deg/sec]. Figure 4.3 is the result of drift estimation by the present method. We use a sixty fourth order FIR digital lowpass filter with a cut-off frequency of 0.2[Hz]. Figure 4.4 shows the rotational angular velocities by the odometry and by the gyroscope with drift compensation. Note that the angular velocity by the odometry( $\Omega_{\text{odom}}(k)$ ) is different from that by the gyroscope( $\bar{\Omega}_{\text{gyro}}(k)$ ) at 15[sec] on account of the sudden error.



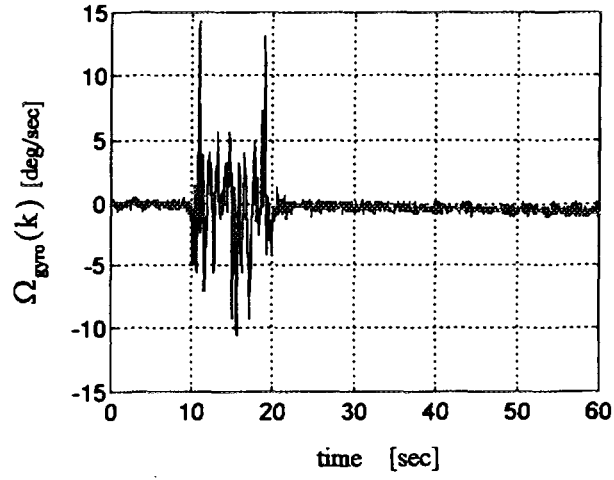


Fig. 4.2 Rotational angular velocity of robot measured by gyroscope.

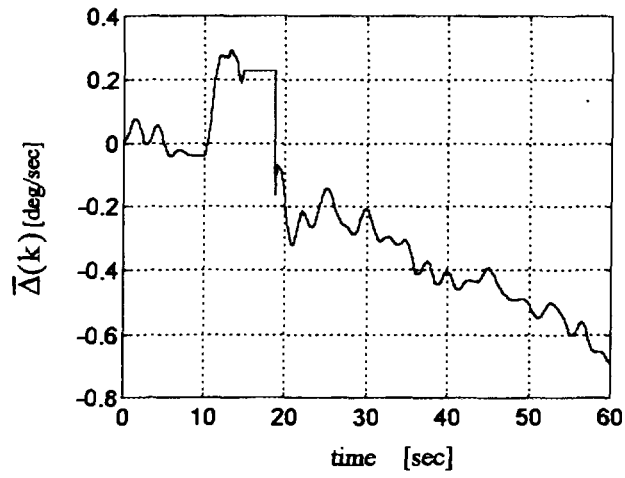


Fig. 4.3 Drift estimation by lowpass filter

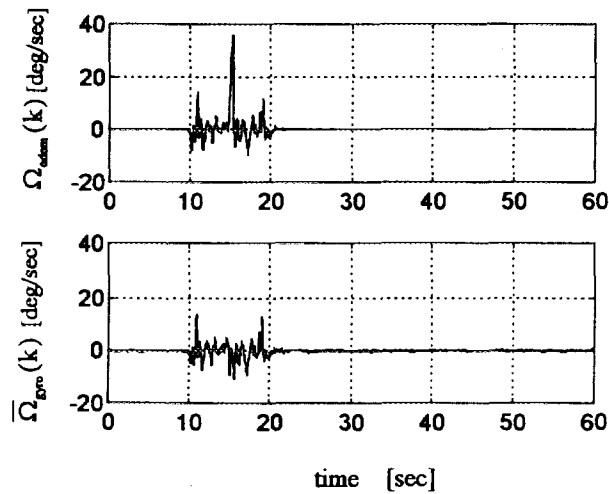


Fig. 4.4 Rotational angular velocities of robot obtained by odometry (top) and measured by gyroscope (bottom)

Figure 4.5 shows the result of position estimation only by the odometry (dashed line) and the combined use of odometry and gyroscope (solid line). Estimated position is updated every 50[msec]. One see that the estimation only by the odometry begins to deviate from a straight line after the sudden error is occurred. The estimation at the goal point is (1720[mm], 215[mm], 15.9[deg]). In the case of combined use of the gyroscope with  $\Delta_{max}$  of 5[deg/sec] by taking account of the noise fluctuation in  $\Omega_{gyro}(k)$ , the estimation is (1749[mm], -34[mm], -1.4[deg]). The orientation angle estimation error in the latter case is found to be reduced to one tenth as compared with the former case.

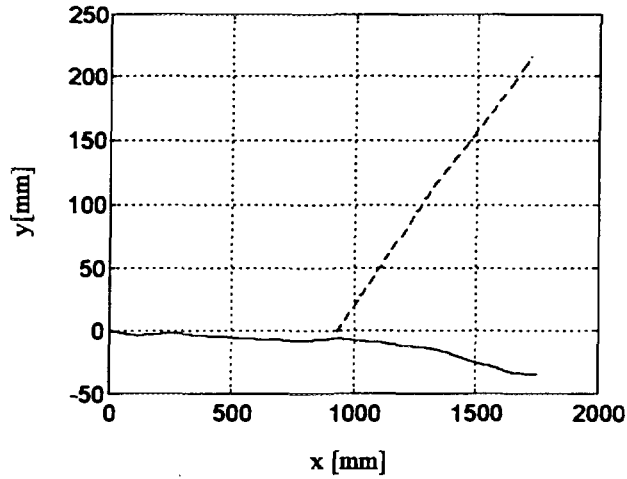


Fig. 4.5 Result of the position estimation by odometry (dashed line) and the combined use of odometry and gyroscope (solid line)

## 4.2 Correction of Position Estimation Error by Using TV Image Deviation

### 4.2.1 Principle

This method uses the difference between actual TV image from the robot-existing position and image generated on the base of the position estimated by internal sensor. To detect the difference we adopt the deviations of the corresponding apexes of object in those images. Figure 4.6 shows coordinate systems for the formulation of this method.

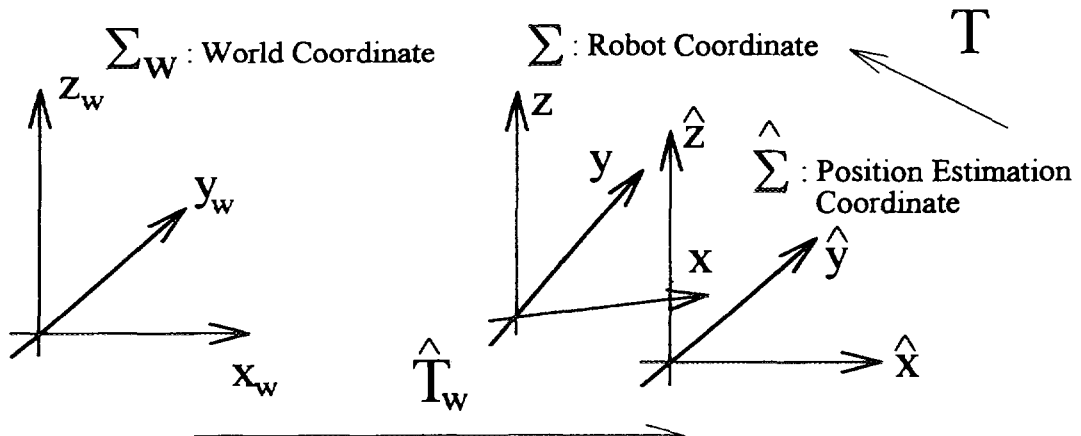


Fig. 4.6 Coordinate system for the estimation error correction

Feature points(apexes) of object represented by the world coordinate system is given as

$${}^w \vec{r}_{obj}^{(i)} = ({}^w x_{obj}^{(i)}, {}^w y_{obj}^{(i)}, {}^w z_{obj}^{(i)}, 1)^T \quad (i=1,2, \dots, N) \quad (10)$$

Let  $(\hat{x}_{rob}, \hat{y}_{rob}, \hat{\theta}_{rob})$  denote the position of robot estimated by the internal sensor. We define the position estimation coordinate system  $\hat{\Sigma}$ , which has the origin at  $(\hat{x}_{rob}, \hat{y}_{rob}, \hat{\theta}_{rob})$ . Feature points of object in the  $\hat{\Sigma}$  is obtained as

$$\hat{r}_{obj}^{(i)} = \hat{T}_w \cdot {}^w \vec{r}_{obj}^{(i)}, \quad (11)$$

where  $\hat{r}_{obj}^{(i)} = (\hat{x}_{obj}^{(i)}, \hat{y}_{obj}^{(i)}, \hat{z}_{obj}^{(i)}, 1)^T$  and

$$\hat{T}_w = \begin{bmatrix} \cos \hat{\theta}_{rob} & \sin \hat{\theta}_{rob} & 0 & -\hat{x}_{rob} \\ -\sin \hat{\theta}_{rob} & \cos \hat{\theta}_{rob} & 0 & -\hat{y}_{rob} \\ 0 & 0 & 1 & 0 \\ 0 & 0 & 0 & 1 \end{bmatrix}. \quad (12)$$

By a pin hole model of camera, feature points of generated image is obtained as

$$\hat{u}_{PX}^{(i)} = \frac{\alpha f \hat{y}_{obj}^{(i)}}{\hat{x}_{obj}^{(i)}}, \quad \hat{v}_{PX}^{(i)} = \frac{\alpha f \hat{z}_{obj}^{(i)}}{\hat{x}_{obj}^{(i)}}, \quad (13)$$

where  $f$  is the focal length of camera lens and  $\alpha$  is the cell size of image plane.

Let  $(x_{rob}, y_{rob}, \theta_{rob})$  denote the actual position of a robot in the world coordinate system. We postulate that this position can be expressed as  $(\hat{x}_{rob} + \Delta x_{rob}, \hat{y}_{rob} + \Delta y_{rob}, \hat{\theta}_{rob} + \Delta \theta_{rob})$ , where  $\Delta x_{rob}$ ,  $\Delta y_{rob}$  and  $\Delta \theta_{rob}$  represent the

position estimation errors. Our objective is to determine  $\Delta x_{\text{rob}}$ ,  $\Delta y_{\text{rob}}$  and  $\Delta\theta_{\text{rob}}$  from the deviations of the corresponding feature points between the TV image and the generated image. We define another coordinate system  $\Sigma$ , called robot coordinate system, the origin of which is at  $(x_{\text{rob}}, y_{\text{rob}}, \theta_{\text{rob}})$ . Feature points of object in the  $\Sigma$  is given as

$$\bar{\mathbf{r}}_{\text{obj}}^{(i)} = \mathbf{T} \cdot \hat{\mathbf{r}}_{\text{obj}}^{(i)}, \quad (14)$$

where  $\hat{\mathbf{r}}_{\text{obj}}^{(i)} = (x_{\text{obj}}^{(i)}, y_{\text{obj}}^{(i)}, z_{\text{obj}}^{(i)}, 1)^T$  and

$$\mathbf{T} = \begin{bmatrix} \cos \Delta\theta_{\text{rob}} & \sin \Delta\theta_{\text{rob}} & 0 & -\Delta x_{\text{rob}} \\ -\sin \Delta\theta_{\text{rob}} & \cos \Delta\theta_{\text{rob}} & 0 & -\Delta y_{\text{rob}} \\ 0 & 0 & 1 & 0 \\ 0 & 0 & 0 & 1 \end{bmatrix}. \quad (15)$$

Therefore, feature points on TV image is represented as

$$\begin{aligned} u_{\text{PX}}^{(i)} &= \frac{\alpha f y_{\text{obj}}^{(i)}}{x_{\text{obj}}^{(i)}} \\ &= \frac{\alpha f (-\hat{x}_{\text{obj}}^{(i)} \sin \Delta\theta_{\text{rob}} + \hat{y}_{\text{obj}}^{(i)} \cos \Delta\theta_{\text{rob}} - \Delta y_{\text{rob}})}{\hat{x}_{\text{obj}}^{(i)} \cos \Delta\theta_{\text{rob}} + \hat{y}_{\text{obj}}^{(i)} \sin \Delta\theta_{\text{rob}} - \Delta x_{\text{rob}}} \\ &\approx g^{(i)}(\Delta x_{\text{rob}}, \Delta y_{\text{rob}}, \Delta\theta_{\text{rob}}) \end{aligned} \quad (16)$$

$$\begin{aligned} v_{\text{PX}}^{(i)} &= \frac{\alpha f z_{\text{obj}}^{(i)}}{x_{\text{obj}}^{(i)}} \\ &= \frac{\alpha f \hat{z}_{\text{obj}}^{(i)}}{\hat{x}_{\text{obj}}^{(i)} \cos \Delta\theta_{\text{rob}} + \hat{y}_{\text{obj}}^{(i)} \sin \Delta\theta_{\text{rob}} - \Delta x_{\text{rob}}} \\ &\approx h^{(i)}(\Delta x_{\text{rob}}, \Delta y_{\text{rob}}, \Delta\theta_{\text{rob}}) \end{aligned} \quad (17)$$

Linearizing the above two equations around  $\Delta x_{\text{rob}} = 0, \Delta y_{\text{rob}} = 0$  and  $\Delta \theta_{\text{rob}} = 0$  yields;

$$\begin{bmatrix} \Delta u_{\text{PX}}^{(i)} \\ \Delta v_{\text{PX}}^{(i)} \end{bmatrix} = \begin{bmatrix} \frac{\partial g^{(i)}}{\partial (\Delta x_{\text{rob}})} & \frac{\partial g^{(i)}}{\partial (\Delta y_{\text{rob}})} & \frac{\partial g^{(i)}}{\partial (\Delta \theta_{\text{rob}})} \\ \frac{\partial h^{(i)}}{\partial (\Delta x_{\text{rob}})} & \frac{\partial h^{(i)}}{\partial (\Delta y_{\text{rob}})} & \frac{\partial h^{(i)}}{\partial (\Delta \theta_{\text{rob}})} \end{bmatrix} \begin{bmatrix} \Delta x_{\text{rob}} \\ \Delta y_{\text{rob}} \\ \Delta \theta_{\text{rob}} \end{bmatrix} \quad (18)$$

where  $\Delta u_{\text{PX}}^{(i)} = u_{\text{PX}}^{(i)} - \hat{u}_{\text{PX}}^{(i)}, \Delta v_{\text{PX}}^{(i)} = v_{\text{PX}}^{(i)} - \hat{v}_{\text{PX}}^{(i)}$ . We simply express this equation as

$$\Delta U_{\text{PX}} = A \Delta r_{\text{rob}} \quad (19)$$

Jacobian matrix A can be obtained as

$$\begin{aligned} A &= \begin{bmatrix} \frac{\partial g^{(i)}}{\partial (\Delta x_{\text{rob}})} & \frac{\partial g^{(i)}}{\partial (\Delta y_{\text{rob}})} & \frac{\partial g^{(i)}}{\partial (\Delta \theta_{\text{rob}})} \\ \frac{\partial h^{(i)}}{\partial (\Delta x_{\text{rob}})} & \frac{\partial h^{(i)}}{\partial (\Delta y_{\text{rob}})} & \frac{\partial h^{(i)}}{\partial (\Delta \theta_{\text{rob}})} \end{bmatrix}_{\Delta r_{\text{rob}}=0} \\ &= \begin{bmatrix} \frac{\alpha \hat{y}_{\text{obj}}^{(i)}}{(\hat{x}_{\text{obj}}^{(i)})^2} & -\frac{\alpha f}{\hat{x}_{\text{obj}}^{(i)}} & -\frac{\alpha f [(\hat{x}_{\text{obj}}^{(i)})^2 + (\hat{y}_{\text{obj}}^{(i)})^2]}{(\hat{x}_{\text{obj}}^{(i)})^2} \\ \frac{\alpha f (\hat{z}_{\text{obj}}^{(i)})^2}{(\hat{x}_{\text{obj}}^{(i)})^2} & 0 & -\frac{\alpha f \hat{y}_{\text{obj}}^{(i)} \hat{z}_{\text{obj}}^{(i)}}{(\hat{x}_{\text{obj}}^{(i)})^2} \end{bmatrix} \end{aligned} \quad (20)$$

From the simultaneous equation of Eq.(19), we can obtain  $\Delta r_{\text{rob}}$  for error correction.

#### 4.2.2 Results of Numerical Simulation

We perform numerical simulation to show the effectiveness of the above

method. As a simulation setup, we presume that the estimated position of the robot by internal sensor is the origin of the world coordinate system and the feature points for error correction are the apexes of the square whose side is 75[mm]. The object (square) is placed at (2000[mm],0,0) in the world coordinate system. In this simulation we choose  $\alpha f=2834.7$ [pixels] as a camera parameter and put the robot at positions apart from the origin of the world coordinate system. Results of the numerical simulation is given in Table 4.1. This reveals that the error correction can be made within 20% uncertainty of initial error and this method has high feasibility as an error correction technique.

Table 4.1 Result of error correction

Deviation from estimated position ( $\Delta x_{\text{rob}}, \Delta y_{\text{rob}}, \Delta \theta_{\text{rob}}$ )	Deviation obtained from error correction method
(100[mm],0,0)	(105.3[mm],0,0)
(0,100[mm],0)	(0,100.0[mm],0)
(0,0,5[deg])	(11.5[mm],-0.7[mm],5.0[deg])
(100[mm],-100[mm],5[deg])	(113.3[mm],-116.2[mm],5.6[deg])

### 4.3 Positioning Tool

Figure 4.7 shows the flowchart of the error correction procedure described in the previous section. This method requires the corresponding of feature points between the actual TV image and the generated image. This corresponding is performed by human to reduce the computational burden of image recognition. The positioning tool is not only the tool for calculating the robot position but also provides the convenient human interface to facilitate the human collaborative procedure such as a feature point correspondence.

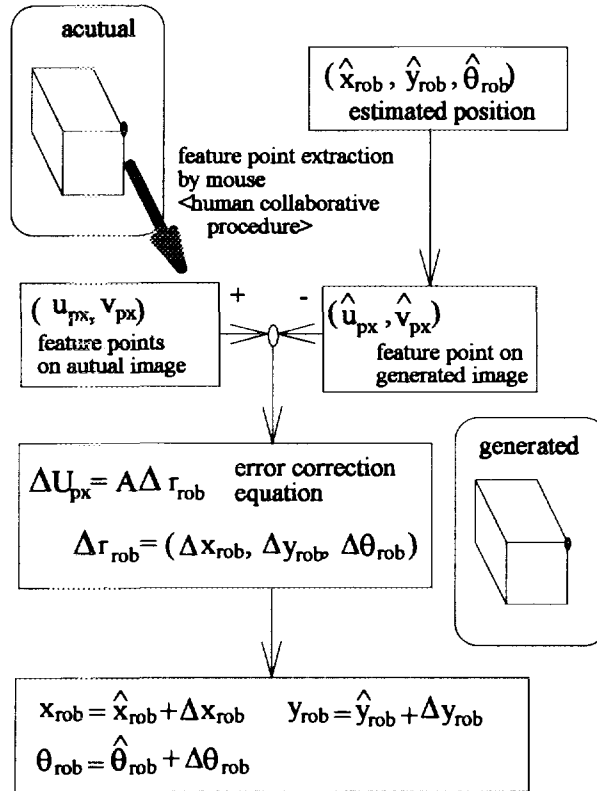


Fig. 4.7 Flowchart of positioning error correction



## 5 Conclusions

As concerns the introduction of mobile robot system for inspecting patrol of nuclear power plants, we proposed the human and robot collaborative system with high efficiency, reliability and safety. To facilitate the human-robot collaboration, the conventional autonomous robot system is improved with sophisticated software such as a server program and an autonomous navigation program. As applicable technologies to the system, two position estimation methods were proposed. One utilizes a gyroscope and the other TV image. The evaluation of their effectiveness and feasibility was made by experiment and numerical simulation. The position estimation by utilization of the gyroscope together with the odometry is ten times better in accuracy than that of the odometry only. By the utilization of TV image, the initial position estimation error can be corrected within 20% uncertainty.

## Acknowledgments

The authors would like to express sincere thanks to Prof. Yuta and Mr. Maeyama of Tsukuba University for their helpful discussion on position estimation with gyroscope. The authors also would like to thank Mr. Furukawa of KCS Corp. for his contributions to autonomous navigation programming. The authors would finally like to express the gratitude to Dr. Ara of Sensing Technology Laboratory for his comments to the manuscript.

## References

- [1] S. Yuta, K. Nagatani and S. Maeyama, “Realizing a Robust Navigation Function on a Small Size Autonomous Mobile Robot”, Proceedings of International Workshop on Some Critical Issues in Robotics, 1995
- [2] H. Yamasaki, “Optimization of Man-machine Role Allocation in Automatic Systems, Journal of SICE, Vol. 35, pp. 571-574, 1996 (in Japanese)
- [3] N. Ishikawa, S. Maeyama, S. Yuta and K. Suzuki, “Experimental Evaluation on Position Estimation of Mobile Robot by the Combined Use of Odometry and Gyro”, JAERI-Research, 97-033, 1997 (in Japanese)
- [4] S. Maeyama, N. Ishikawa and S. Yuta, “Rule Based Filtering and Fusion of Odometry and Gyroscope for a Fail safe Dead Reckoning System for a Mobile Robot”, Proceedings of the 1996 International Conference on Multisensor Fusion and Integration for Intelligent Systems, pp. 541-548, 1996

# 国際単位系 (SI) と換算表

表1 SI基本単位および補助単位

量	名称	記号
長さ	メートル	m
質量	キログラム	kg
時間	秒	s
電流	アンペア	A
熱力学温度	ケルビン	K
物質質量	モル	mol
光度	カンデラ	cd
平面角	ラジアン	rad
立体角	ステラジアン	sr

表2 SIと併用される単位

名称	記号
分, 時, 日	min, h, d
度, 分, 秒	°, ', "
リットル	l, L
トン	t
電子ボルト	eV
原子質量単位	u

$1 \text{ eV} = 1.60218 \times 10^{-19} \text{ J}$   
 $1 \text{ u} = 1.66054 \times 10^{-27} \text{ kg}$

表5 SI接頭語

倍数	接頭語	記号
$10^{18}$	エクサ	E
$10^{15}$	ペタ	P
$10^{12}$	テラ	T
$10^9$	ギガ	G
$10^6$	メガ	M
$10^3$	キロ	k
$10^2$	ヘクト	h
$10^1$	デカ	da
$10^{-1}$	デシ	d
$10^{-2}$	センチ	c
$10^{-3}$	ミリ	m
$10^{-6}$	マイクロ	$\mu$
$10^{-9}$	ナノ	n
$10^{-12}$	ピコ	p
$10^{-15}$	フェムト	f
$10^{-18}$	アト	a

表3 固有の名称をもつSI組立単位

量	名称	記号	他のSI単位による表現
周波数	ヘルツ	Hz	$\text{s}^{-1}$
力	ニュートン	N	$\text{m}\cdot\text{kg}/\text{s}^2$
圧力, 応力	パスカル	Pa	$\text{N}/\text{m}^2$
エネルギー, 仕事, 熱量	ジュール	J	$\text{N}\cdot\text{m}$
工率, 放射束	ワット	W	$\text{J}/\text{s}$
電気量, 電荷	クーロン	C	$\text{A}\cdot\text{s}$
電位, 電圧, 起電力	ボルト	V	$\text{W}/\text{A}$
静電容量	ファラド	F	$\text{C}/\text{V}$
電気抵抗	オーム	$\Omega$	$\text{V}/\text{A}$
コンダクタンス	ジーメン	S	$\text{A}/\text{V}$
磁束	ウェーバ	Wb	$\text{V}\cdot\text{s}$
磁束密度	テスラ	T	$\text{Wb}/\text{m}^2$
インダクタンス	ヘンリー	H	$\text{Wb}/\text{A}$
セルシウス温度	セルシウス度	$^{\circ}\text{C}$	
光束	ルーメン	lm	$\text{cd}\cdot\text{sr}$
照度	ルクス	lx	$\text{lm}/\text{m}^2$
放射能	ベクレル	Bq	$\text{s}^{-1}$
吸収線量	グレイ	Gy	$\text{J}/\text{kg}$
線量当量	シーベルト	Sv	$\text{J}/\text{kg}$

表4 SIと共に暫定的に維持される単位

名称	記号
オングストローム	$\text{\AA}$
バ	b
バール	bar
ガリ	Gal
キュリー	Ci
レントゲン	R
ラド	rad
レム	rem

$1 \text{ \AA} = 0.1 \text{ nm} = 10^{-10} \text{ m}$   
 $1 \text{ b} = 100 \text{ fm} = 10^{-28} \text{ m}^2$   
 $1 \text{ bar} = 0.1 \text{ MPa} = 10^5 \text{ Pa}$   
 $1 \text{ Gal} = 1 \text{ cm}/\text{s}^2 = 10^{-2} \text{ m}/\text{s}^2$   
 $1 \text{ Ci} = 3.7 \times 10^{10} \text{ Bq}$   
 $1 \text{ R} = 2.58 \times 10^{-4} \text{ C}/\text{kg}$   
 $1 \text{ rad} = 1 \text{ cGy} = 10^{-2} \text{ Gy}$   
 $1 \text{ rem} = 1 \text{ cSv} = 10^{-2} \text{ Sv}$

(注)

- 表1-5は「国際単位系」第5版, 国際度量衡局 1985年刊行による。ただし, 1 eV および 1 uの値は CODATAの1986年推奨値によった。
- 表4には海里, ノット, アール, ヘクタールも含まれているが日常の単位なのでここでは省略した。
- barは, JISでは流体の圧力を表わす場合に限り表2のカテゴリーに分類されている。
- EC閣僚理事会指令では bar, barnおよび「血圧の単位」mmHgを表2のカテゴリーに入れている。

## 換 算 表

力	N(=10 <sup>5</sup> dyn)	kgf	lbf
	1	0.101972	0.224809
	9.80665	1	2.20462
	4.44822	0.453592	1

粘 度 1 Pa·s(N·s/m<sup>2</sup>)=10 P(ポアズ)(g/(cm·s))

動粘度 1 m<sup>2</sup>/s=10<sup>4</sup>St(ストークス)(cm<sup>2</sup>/s)

圧	MPa(=10 bar)	kgf/cm <sup>2</sup>	atm	mmHg(Torr)	lbf/in <sup>2</sup> (psi)
	1	10.1972	9.86923	7.50062 × 10 <sup>2</sup>	145.038
力	0.0980665	1	0.967841	735.559	14.2233
	0.101325	1.03323	1	760	14.6959
	1.33322 × 10 <sup>-4</sup>	1.35951 × 10 <sup>-3</sup>	1.31579 × 10 <sup>-3</sup>	1	1.93368 × 10 <sup>-2</sup>
	6.89476 × 10 <sup>-3</sup>	7.03070 × 10 <sup>-2</sup>	6.80460 × 10 <sup>-2</sup>	51.7149	1

エネルギー・仕事・熱量	J(=10 <sup>7</sup> erg)	kgf·m	kW·h	cal(計量法)	Btu	ft·lbf	eV	1 cal = 4.18605 J(計量法)
	1	0.101972	2.77778 × 10 <sup>-7</sup>	0.238889	9.47813 × 10 <sup>-4</sup>	0.737562	6.24150 × 10 <sup>18</sup>	= 4.184 J (熱化学)
	9.80665	1	2.72407 × 10 <sup>-6</sup>	2.34270	9.29487 × 10 <sup>-3</sup>	7.23301	6.12082 × 10 <sup>19</sup>	= 4.1855 J (15 °C)
	3.6 × 10 <sup>6</sup>	3.67098 × 10 <sup>5</sup>	1	8.59999 × 10 <sup>5</sup>	3412.13	2.65522 × 10 <sup>6</sup>	2.24694 × 10 <sup>25</sup>	= 4.1868 J(国際蒸気表)
	4.18605	0.426858	1.16279 × 10 <sup>-6</sup>	1	3.96759 × 10 <sup>-3</sup>	3.08747	2.61272 × 10 <sup>19</sup>	仕事率 1 PS(仏馬力)
	1055.06	107.586	2.93072 × 10 <sup>-4</sup>	252.042	1	778.172	6.58515 × 10 <sup>21</sup>	= 75 kgf·m/s
	1.35582	0.138255	3.76616 × 10 <sup>-7</sup>	0.323890	1.28506 × 10 <sup>-3</sup>	1	8.46233 × 10 <sup>18</sup>	= 735.499 W
	1.60218 × 10 <sup>-19</sup>	1.63377 × 10 <sup>-20</sup>	4.45050 × 10 <sup>-26</sup>	3.82743 × 10 <sup>-20</sup>	1.51857 × 10 <sup>-22</sup>	1.18171 × 10 <sup>-19</sup>	1	

放射能	Bq	Ci
	1	2.70270 × 10 <sup>-11</sup>
	3.7 × 10 <sup>10</sup>	1

吸収線量	Gy	rad
	1	100
	0.01	1

照射線量	C/kg	R
	1	3876
	2.58 × 10 <sup>-4</sup>	1

線量当量	Sv	rem
	1	100
	0.01	1

